CHINA FOUNDRY Research & Development
Vol. 20 No. 6 November 2023
www.springer.com/41230
https://doi.org/10.1007/s41230-023-3057-7

Analysis of inhomogeneity of solidified microstructure of continuous casting copper tubular billet based on factor analysis

Jin-song Liu[1, 2, 3], Chao-rui Shan[1], *Da-yong Chen[2, 3], Hong-wu Song[2], Chuan-lai Chen[3], and Yun-yue Chen[3]

1. School of Materials Science and Engineering, Shenyang Ligong University, Shenyang 110159, China

2. Shi-Changxu Innovation Center for Advanced Materials, Institute of Metal Research, Chinese Academy of Sciences, Shenyang 110016, China

3. Changzhou Enreach Copper Co., Ltd., Changzhou 213149, Jiangsu, China

Abstract: The horizontal continuous casting process, the initial step in TP2 copper tubular processing, directly determines the microstructure and properties of copper tubular. However, the process parameters of the continuous casting characterize time variation, multiple disturbances and strong coupling. As a consequence, their influence on a casting billet is difficult to be determined. Due to the above issues, the common factor and special factor analysis of the factor analysis model were used in this study, and the casting experiment and billet metallographic experiment were carried out to diagnose and analyze the reason of the microstructure inhomogeneity. The multiple process parameters were studied and classified using common factor analysis, the cast billets with abnormal microstructures were identified by GT^2 statistics, and the most important factors affecting the microstructural homogeneity were found by special factor analysis. The calculated and experimental results show that the principal parameters influencing the inhomogeneity of solidified microstructure are the primary inlet water pressure and the primary outlet water temperature. According to the consequence of the above investigation, the inhomogeneity of the copper billet microstructure can be effectively improved when the process parameters are controlled and adjusted.

Keywords: TP2 copper tubular billet; horizontal continuous casting; factor analysis; microstructure inhomogeneity of casting billet; quality diagnosis

CLC numbers: TG146.1+1 **Document code:** A **Article ID:** 1672-6421(2023)06-526-11

1 Introduction

Horizontal continuous casting (HCC) process, the initial step in the casting and rolling process of copper tube with high precision, is characterized by multi-physical field coupling, multi-factor influences and multi-disturbance variations. The microstructure of the cast billet influences the forming ability and mechanical properties of the products [1-2]. The investigation from the University of Science and Technology Beijing showed that the microstructure of special orientations directly influenced the mechanical properties. For instance, the high orientation, the flat small-angle grain boundaries and more <001> soft orientation structure [3]. It indicated that the microstructure of the casting billet and its homogeneity had a significant influence on the subsequent forming properties of the billet and even the quality of the final product [3]. Edosa et al. [4] outlined the influence of process parameters on the mechanical properties and microstructure of castings during extrusion casting, and identified the most influential parameters were extrusion pressure, casting temperature, and mold temperature, and gave the corresponding optimal parameter ranges. Hu et al. [5] studied the effect of specific cooling conditions on the microstructure and mechanical properties of A356 castings after T6 heat treatment. The results showed that the subcooling degree was closely related to the temperature of the mold and pouring. The specimens exhibited better mechanical properties when the temperature of the mold was 270 °C and pouring at 680 °C. Li et al. [6] investigated the effects of continuous casting process parameters on the secondary dendritic arm spacing, equiaxed crystal rate, and average grain size of the microstructure of GCr15 bloom alloy, and proposed

***Da-yong Chen**

Male, born in 1987, Ph.D., Assistant Professor. Main research fields: the mechanism of plasticity enhancement of non-ferrous metals and intelligent manufacturing of tubular and platelike component of non-ferrous metals.

E-mail: dychen15b@imr.ac.cn

Received: 2023-05-09; Accepted: 2023-09-10

the optimal process parameters to improve the central carbon segregation. Chen et al. [7] studied the microstructure and microhardness of Ti-48Al alloy at different cooling rates, and found that the average size of the lamellar cluster and lamellar spacing decreased as the cooling rate increased, thus increasing the microhardness of Ti-48Al alloy. However, the process such as HCC is complex and the microstructure of the casting billet is influenced by various process variables. Therefore, it is of great importance to establish the relationship between the process parameters of the horizontal continuous casting and its casting microstructure to ensure the process variables within a reasonable range, so as to achieve the improvement of the quality of the billet.

Fault diagnosis is widely used in industrial production as a method to detect and locate the occurrence and location of faults, which can be mainly divided into analytical model and data-driven fault diagnosis methods. Fault diagnosis based on an analytical model requires an accurate mathematical model, which is difficult to establish for complex systems with unclear mechanisms [8]. In this case, a data-driven fault diagnosis method is adopted for effective fault diagnosis of the horizontal continuous casting process, i.e., for analysis of the factors affecting the quality of the cast billets. Data-driven fault diagnosis can be accomplished based on production data without need of establishing an accurate analytical model, and it is currently becoming a hot spot for contemporary fault diagnosis research [9-10]. Principal component analysis (PCA) is the most widely used multivariate and statistical analysis method among various data-driven fault diagnosis methods [11]. Peng et al. [12] used PCA to accurately predicted the fracture of the submersible oil electric pump shaft based on the two-dimensional diagram of the principal component scores. The PCA model was firstly improved and applied to diagnose the defects in timber in combination with SPE diagnosis by Tafarroj et al. [13], in which, its good accuracy and reliability was fully demonstrated. Gu et al. [14] proposed the PCA and the support vector machine (SVM) fault diagnosis method to achieve dimensionality reduction of fault features, and improve diagnostic efficiency and accuracy. A partitioned principal component analysis (PPCA) method was proposed by Wang et al. [15] and applied to the identification of fault variables, which can reflect the local behavior of process changes in the model and improve monitoring performance by combining local monitoring results. A mixed probabilistic principal component analysis (MPPCA) diagnostic method was investigated by Sharifi et al. [16], and it was implemented for the sensor fault monitoring of nonlinear systems. This method aims to improve the accuracy of fault diagnosis by separating the measurement space into several local linear regions. Factor analysis, as an extension of principal meta-analysis, enables the exploration of the primary influencing factors for data downscaling and peacekeeping, compensating for the limitations of principal meta-analysis and gaining wider applications [17]. Zhao et al. [18] proposed a comprehensive monitoring indicator based on the factor analysis model to monitor the controlled state of the process and reduce monitoring indicators. Liu et al. [19] developed the method of contribution graph control limits by expanding the factor analysis monitoring index, which helps to monitor the fault contribution graph and provides a more intuitive basis for system monitoring. In addition, Ding et al. [20] used factor analysis to establish a process monitoring model for rotary kiln faults, and its accuracy on detecting system faults and anomalies was verified. Peng et al. [21] combined factor analysis with GT^2 to monitor the production process, and found that it could identify the causes of defects by characterizing the influence of process parameters on the width of sheet strip based on the factor scores.

Factor analysis was adopted in this study to diagnose the abnormal process parameters of the horizontal continuous casting of TP2 copper tubular billets that caused inhomogenous microstructure based on Python language. Data were collected and standardized by Pandas and Numpy databases within long-term cycles in the horizontal continuous casting process. A series of calculations and analyses were conducted to establish the factor analysis model including computations of method applicability, common factor, sample outlier, factor score, special factor extraction, and influence analysis. The causes of the microstructure inhomogeneity were eventually identified and the verification testing was conducted on key process parameters to improve the quality of cast billets. In this way, it will provide a quantitative basis for the stability of the process, and guarantee for the improvement of product quality.

2 Principle and research scheme of factor analysis

2.1 Fundamental concept of factor analysis

Factor analysis is a multivariate and statistical analysis method based on the correlations of the original data, which uses the mathematical methods to reduce variables with complex relationships to several factors that can represent the original variables [22]. The factor analysis method not only preserves most of the representative information of the original variables in the process of dimensionality reduction, but also can find the major factors influencing the observed targets and reflect the intrinsic connection of the original variables.

2.2 Fundamental principles

A $n\times p$ matrix $X_{n\times p}$ can be constituted for p evaluation dimensions (e.g., different process parameters with p dimensions) if n evaluation samples are collected. The matrix can be expressed as the expression of the matrix of loads, the common factor ($[F_1, F_2\cdots F_m]$), the special factor ($[\varepsilon_1, \varepsilon_2\cdots\varepsilon_p]$) and the expectations, as shown in Eq. (1). The p process variables of the assessment object can be expressed as m (usually $m<p$) common factors if the correlation among the evaluated objects is strong. The common factor retains the categorical features of the evaluated objects to the utmost extent, by which realizes data dimensionality reduction. In addition, the parameters influencing

the evaluated objects mostly can be confirmed among various process parameters by the calculation and analysis of the special factor scores, which can lay a quantitative foundation for the optimization of the process.

$$\begin{bmatrix} X_1 \\ X_2 \\ \vdots \\ X_p \end{bmatrix} = \begin{bmatrix} \mu_1 \\ \mu_2 \\ \vdots \\ \mu_p \end{bmatrix} + \begin{bmatrix} a_{11} & a_{12} \cdots a_{1m} \\ a_{21} & a_{22} \cdots a_{2m} \\ \vdots & \vdots \quad \vdots \\ a_{p1} & a_{p2} \cdots a_{pm} \end{bmatrix} \begin{bmatrix} F_1 \\ F_2 \\ \vdots \\ F_m \end{bmatrix} + \begin{bmatrix} \varepsilon_1 \\ \varepsilon_2 \\ \vdots \\ \varepsilon_p \end{bmatrix} \quad (1)$$

Or $X = \mu + AF + \varepsilon$

where, μ is the expected vector of X, $F=(F_1, F_2, \cdots, F_m)^T$ is the common factor of X where the components are not linearly related to each other, $\varepsilon=(\varepsilon_1, \varepsilon_2, \cdots, \varepsilon_m)$ refers to the special factor of each component of X, and ε_i is independent from the others. In addition, ε_i and F_i are independent from each other.

2.3 Research scheme of factor analysis

In this study, the factor analysis model was adopted to investigate the relationship between the microstructure homogeneity and the casting process parameters, and the overall scheme is illustrated in Fig. 1. Firstly, the collecting and extraction of the data were conducted for the whole process parameters of a copper tubular billet by horizontal continuous casting. Secondly, standardizing of the extracted data was implemented to avoid the influence exerted by the differences in data dimensions and magnitudes. Thirdly, the condition was estimated whether the data was satisfied with factor analysis. Then, the number of factors was determined according to the criteria that the initial eigenvalue of the factors is greater than 1 and the cumulative variance contribution of the factors is greater than 80%. Then, the factor loading matrix was calculated and rotated to meet the categorization of the production process and to calculate the common factor score and the comprehensive factor score. After that, the unusual sample was found out according to the sample outliers. Last but not least, the cause of the unusual phenomenon in the sample is demonstrated by calculating the special factor score.

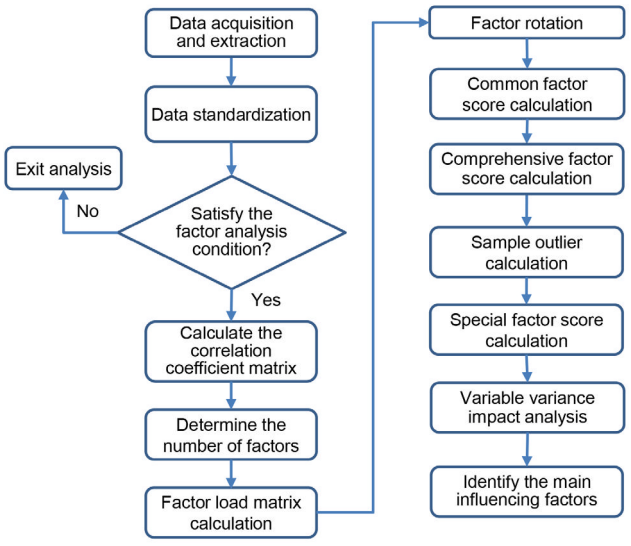

Fig. 1: Research scheme of factor analysis

3 Process data handling

3.1 Data acquisition and extraction

Horizontal continuous casting of copper tubular billets mainly consists of several steps as follows: Firstly, the A-grade electrolytic copper plates (copper content was not less than 99.9935%) were melted completely in the melting furnace. Secondly, the copper liquid flowed into the holding furnace through the flow trough and then it flowed into the graphite crystallizer through the liquid inlet under gravity. Then, under the cooling effect of primary cooling water, the copper liquid began to solidify, gradually forming the initial solidification shell with a certain thickness. The solidified copper was drawn out by the traction machine. Then, the secondary cooling water was sprayed directly on the outer surface of the billet to further solidify it until the formation of a complete billet. Finally, the billet was cut by the sawing machine when it reached a certain length [23-24].

Ten process parameters were included in this study: temperature of liquid copper in the holding furnace, withdrawal speed, primary inlet water pressure, primary inlet water temperature, primary outlet water temperature 1, primary outlet water temperature 2, primary inlet water flow rate 1, primary inlet water flow rate 2, primary outlet water flow rate 1, primary outlet water flow rate 2. The numbers 1 and 2 after 'inlet water flow' correspond to the upper and lower part of the crystallizer, which were saved in the WinCC system.

The S-type thermocouple was used to measure the temperature of the liquid copper. The pressure gauge was adopted to collect the primary inlet water pressure which was installed in the main pipe of the inlet water. Furthermore, temperature sensors were installed in the sub pipeline to obtain the data of the primary inlet water temperature, primary outlet water temperature 1, and primary outlet water temperature 2. Meanwhile, turbine flowmeters were employed to collect the data of the primary inlet water flow rate 1, primary inlet water flow rate 2, primary outlet water flow rate 1, and primary outlet water flow rate 2. The measuring devices and their types are listed in Table 1. The collected data were converted to the floating version by the corresponding converter and the PLC, and were finally saved in the different modules of the WinCC system.

The solidification process was completed when the sawing machine cut off the specimen, which exists a time difference between the process parameters and the detection of the cast billet microstructure. Consequently, an automatic processing program was designed to find out the sawing time from the data stored in system of WinCC. On the one hand, the sawing time was treated as the medium to match the continuous casting number. On the other hand, the microstructure could correspond with casting process parameters if the casting time and parameters were found out based on the sawing time. The principle of horizontal continuous casting of copper tubular billet and the relationship of data acquisition are illustrated in Fig. 2.

The data of the process variables during the horizontal continuous casting of copper tubular billets were saved in

Table 1: Devices and types for process parameter acquisition

Process parameter	Devices	Types
Withdrawal speed (mm·min^{-1})	Tractor	GYT4-QY-HY
Temperature of liquid copper (°C)	Thermocouple	S-Thermocouple
Primary inlet water pressure (MPa)	Pressure transfer controller	MPM484C
Primary inlet/outlet water temperature (°C)	Temperature transmitter	MTMK5883
Primary inlet/outlet water flow (L·min^{-1})	Turbine flowmeter	LWGY-020-OLE-N-Ib-TcPc-NV1

the database of the WinCC system. The rapid filter and dealing system were utilized to export and handle the data from the WinCC system to avoid the abundant noise, testing error and data loss because of the complexity of the industrial system and the unsatisfactory running environment. The average value of the data within 5 min was used as the sample data to ensure the stability and applicability, and avoid the influence of data noise on the analysis results. The data of horizontal continuous casting process parameters are shown in Table 2.

3.2 Data processing

One sample was obtained if the p process variables X_1, $X_2 \cdots X_p$ were collected. An $n \times p$ dimensional matrix $X_{n\times p}$ was realized if n collections were made:

$$X_{n\times p} = \begin{bmatrix} X_{11} & X_{12} \cdots X_{1p} \\ X_{21} & X_{22} \cdots X_{2p} \\ \vdots & \vdots & \vdots \\ X_{n1} & X_{n2} \cdots X_{np} \end{bmatrix} \quad (2)$$

In a multi-indicator evaluation system, indicators have different dimensions and orders of magnitude depending on their nature. The role of process

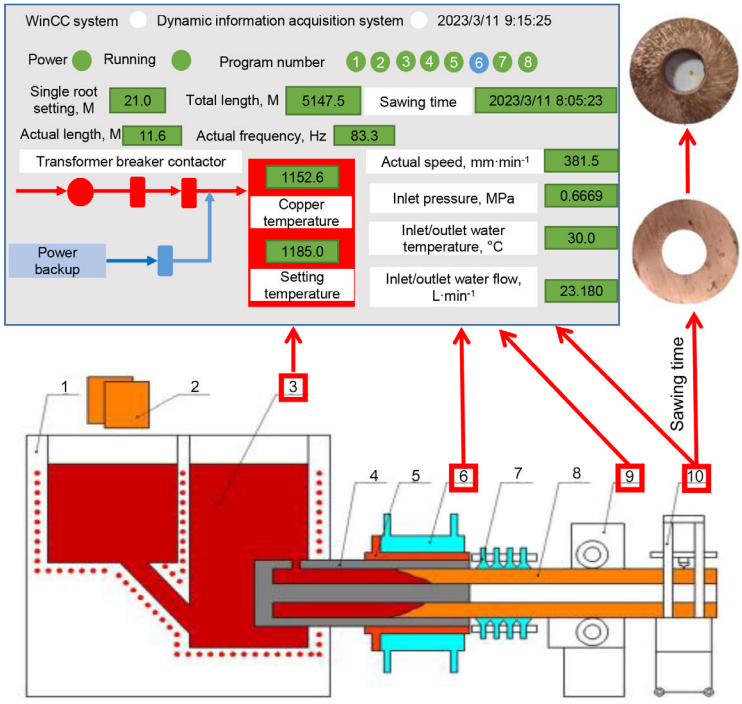

1. Melting furnace; 2. Electrolytic copper plate; 3. Molten copper; 4. Crystallizer; 5. Cooling copper jacket; 6. First cooling zone; 7. Second cooling zone; 8. Copper tubular billet; 9. Traction machine; 10. Sawing machine

Fig. 2: Horizontal continuous casting process and data acquisition diagram

Table 2: Process parameters of horizontal continuous casting

Withdrawal speed (mm·min^{-1})	Temperature of liquid copper (°C)	Primary inlet water pressure (MPa)	Primary inlet water temperature (°C)	Primary outlet water temperature 1 (°C)	Primary outlet water temperature 2 (°C)	Primary inlet water flow 1 (L·min^{-1})	Primary inlet water flow 2 (L·min^{-1})	Primary outlet water flow 1 (L·min^{-1})	Primary outlet water flow 2 (L·min^{-1})
308.543	1,178.587	0.6669	24.107	53.997	48.973	23.180	25.170	27.073	21.933
333.237	1,167.727	0.6600	30.000	56.370	56.153	25.000	28.050	29.020	23.460
333.497	1,167.553	0.6541	29.000	53.353	53.360	28.000	30.053	32.670	26.000
...									
383.000	1,164.423	0.6500	29.000	51.000	49.017	11.040	13.000	13.703	12.000
400.040	1,168.363	0.6402	30.000	49.453	47.953	11.493	13.000	13.640	12.000
400.040	1,169.193	0.6400	30.000	50.020	48.673	11.000	13.000	13.510	11.960

parameters with higher values is relatively prominent while the role of process parameters with lower values is relatively weaker in the comprehensive analysis when the difference of indicators is obvious and the analysis is carried out directly under condition of the original data. Differences in magnitudes affect the reliability of the calculated results. Therefore, the original index data should be standardized in order to ensure the reliability of the results which is illustrated as follows:

$$X_{ij}^{*}=\frac{X_{ij}-\overline{X}_{j}}{S_{j}} \tag{3}$$

The standardized data can represent preferably the interrelationships among the variables. The fluctuation change of the variants can be compared more exactly by the calculation of the variance which can avoid the influence of the dimensions on the calculated results.

4 Application and analysis of results

4.1 Suitability test

The prerequisite for conducting factor analysis is that the data need to satisfy the requirement of high correlation. In consequence, the suitability of the data needs to be tested firstly. Two methods were used to test the suitability of data, including KMO (Kaiser-Meyer-Olkin) and Bartlett's inspection. The data are suitable for factor analysis when the general KMO values are greater than 0.5, and its value will be better if it is closer to 1. Bartlett's inspection result P should be less than 0.05. As illustrated in Table 3, the KMO value is 0.710, and the significance value is 0.000 which is less than 0.05 when Bartlett's inspection value is 1,614.363, indicating that the data are suitable for factor analysis.

4.2 Determination of number of common factors

The final variance contributions of the process variables are shown in Table 4 when the factor analysis was performed on the standardized data using PCA. As can be seen, there are 3 factors with initial eigenvalues greater than 1, whose variance contribution rates were 49.268%, 25.582%, and 15.341%, respectively. And the cumulative variance contribution rate of the factors is 90.191%, which means that the three extracted common factors could represent 90.191% of the information of the original 10 variables.

Table 3: KMO and Bartlett tests

KMO		Bartlett's inspection	
Measure of sampling adequacy	0.710	Approx. Chi-Square	1,614.363
		Degree of freedom	45
		Significance	0.000

4.3 Establishment of factor loading matrix

The matrix of the factor analysis model can be expressed as follows:

$$X-\mu=AF+\varepsilon \tag{4}$$

The covariance expression for X and F is shown as:

$$COV(X,F)=COV(AF+\varepsilon,F)=A \tag{5}$$

The covariance matrix $COV(X)$ of X is defined as Σ, satisfying the following relation:

$$\begin{aligned}\Sigma&=COV(X)=COV(AF)+COV(\varepsilon)+COV(AF,\varepsilon)\\&=AA^{\mathrm{T}}+\psi\end{aligned} \tag{6}$$

The estimation of the loading matrix can be performed by the covariance matrix based on the spectral decomposition of Σ from the matrix of Eq. (4) and the expression of the covariance matrix of Eq. (5).

$$\Sigma=\sum_{j=1}^{p}\lambda_j e_j e_j^{T}=\Lambda_{p\times p}\Lambda_{p\times p}^{T} \tag{7}$$

where, $\Lambda=\left(\sqrt{\lambda_1}\,e_1,\cdots,\sqrt{\lambda_p}\,e_p\right)$, (λ_j,e_j) are the eigenvalues and

Table 4: Total variance of interpretation

Variables	Initial eigenvalue			Extraction of squares loading			Rotating sum of squares loading		
	Eigenvalue	Variance (%)	Total (%)	Eigenvalue	Variance (%)	Total (%)	Eigenvalue	Variance (%)	Total (%)
1	4.927	49.268	49.268	4.927	49.268	49.268	4.065	40.655	40.655
2	2.558	25.582	74.850	2.558	25.582	74.850	2.721	27.206	67.861
3	1.534	15.341	90.192	1.534	15.341	90.192	2.233	22.331	90.192
4	0.585	5.849	96.040						
5	0.150	1.504	97.544						
6	0.125	1.249	98.793						
7	0.074	0.737	99.530						
8	0.042	0.418	99.948						
9	0.003	0.027	99.976						
10	0.002	0.024	100.000						

eigenvectors of Σ, respectively. The following equation can be defined if the last p-m eigenvalues are small enough:

$$A=\left(\sqrt{\lambda_1}\,e_1,\cdots,\sqrt{\lambda_m}\,e_m\right) \tag{8}$$

At the sample level, the sample covariance matrix S instead of Σ can be used. Thus, the loading matrix is obtained based on the principal component method.

$\left(\hat{\lambda}_j,\hat{e}_j\right), j=1,\ldots p,$ is the normalized eigenpairs after the covariance matrix S of the sample is sorted. The principal-form decomposition of the factor loading matrix estimation is as Eq. (9) if $m(m<p)$ denotes the number of common factors:

$$\hat{A}=\left(\sqrt{\hat{\lambda}_1}\,\hat{e}_1,\ldots,\sqrt{\hat{\lambda}_m}\,\hat{e}_m\right) \tag{9}$$

The computed factor loading matrix was rotated using the Kaiser normalized maximum variance method. The common factor F1 has larger loadings on variables of 07, 08, 09 and 10, which can be named as water flow factors according to the rotated factor loadings shown in Table 5. Meanwhile, the common factor F2 has larger loadings on variables of 01, 02, 03, and 04, which are named as control factors. Furthermore, the common factor F3 has larger loadings on variables of 05 and 06, which can be entitled outlet water factors. The dimensionality reduction of the process parameters is realized when the common factors are classified and named which can reduce the number of variables, facilitate data processing and estimate the common factors that affect the microstructure.

Table 5: Factor loading table after rotation

Parameters number	Process parameters	Common factor corresponds to the value of loading matrix		
		F1	F2	F3
01	Traction rate		0.793	
02	Temperature of liquid copper		−0.744	
03	Primary inlet water pressure		−0.748	
04	Primary inlet water temperature		0.878	
05	Primary outlet water temperature 1			0.926
06	Primary outlet water temperature 2			0.943
07	Primary inlet water flow 1	0.981		
08	Primary inlet water flow 2	0.977		
09	Primary outlet water flow 1	0.970		
10	Primary outlet water flow 2	0.957		

4.4 Monitoring and diagnosis of casting process

GT^2 statistics and factor scores can also be defined in factor analysis model for monitoring the main and special factor spaces which is similar to the definition of T^2 monitoring metrics in PCA monitoring.

The principal factors obey a standard normal distribution with unit variance [19] as follows:

$$GT^2=f^T f\sim X^2(k) \tag{10}$$

where, k is the number of factors selected, the control limit expresses as $CGT^2=X^2_{1-\alpha}(k)$, α is the saliency. The score of special factors ε_i can be calculated from the factor model $X=\mu+AF+\varepsilon$. There will be an abnormity in the common factor space when the GT^2 statistic exceeds the control limit [20]. Eighty-nine sample data were selected for production process monitoring, and the monitoring results with the control limits of the samples at 97% confidence level are shown in Fig. 3.

It is easy to see that Samples No. 1, No. 2, No. 45 and No. 46 exceed the control limits, showing that the process parameters corresponding to these four samples are abnormal.

The corresponding metallographic microstructure results of Samples No. 1, No. 2, No. 45 and No. 46 are shown in Figs. 4(a), (b), (c) and (d). The microstructure of standard cast billets is shown in Figs. 4(e) and (f). The standard microstructure of the casting billet has no coarse grains, and the grains are homogenous from the circumferential direction and characterize obvious central symmetry. The equivalent grain width is about 1–2 mm, and the grains are fine. By comparing the structure with the standard of casting billet,

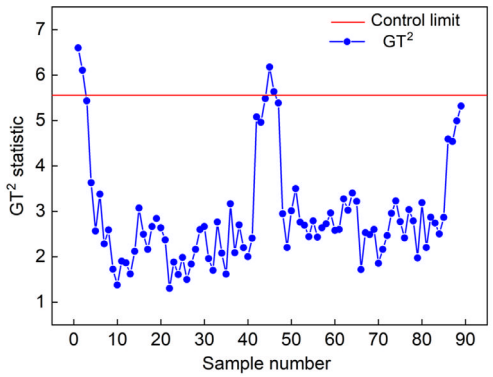

Fig. 3: Error statistics of microstructure defects in factor analysis

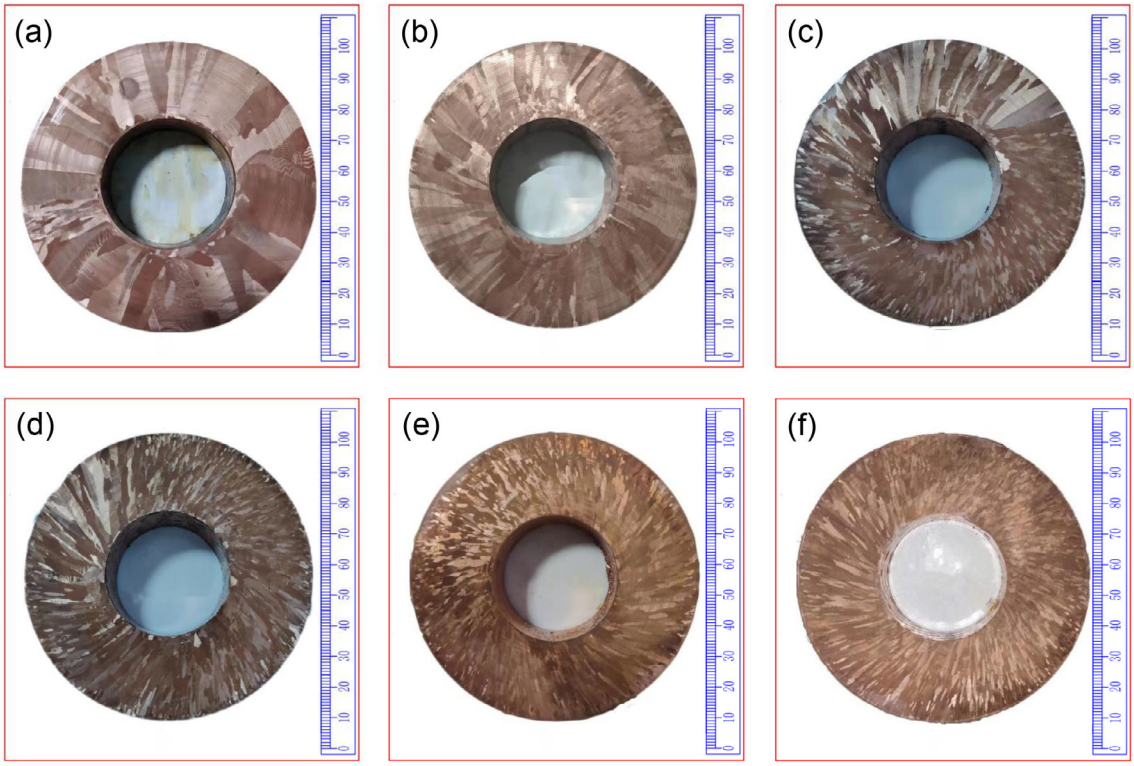

Fig. 4: Metallographic microstructure diagram: (a) Sample 1; (b) Sample 2; (c) Sample 45; (d) Sample 46; (e) Standard microstructure 1; (f) Standard microstructure 2

it is observed that the microstructure of the cast billets in Figs. 4(a) and (b) shows obvious coarse grains. Furthermore, there is only one grain in most positions along the direction of wall thickness, and the equivalent width of the grains is approximate in the range of 5 mm–10 mm. Moreover, the microstructure has obvious asymmetric characteristics: it is coarse in the upper part of the cast billets and fine in the lower part, as illustrated in Figs. 4(c) and (d). Moreover, the lower part of the cast billets has 2–3 groups of grains in the thickness direction of the lower half of the billet, and the upper half has only one group of grains in the radial direction at many positions. The inhomogenous microstructure is found for the casting billet under such process parameters after the comprehensive analysis listed as above.

In order to further analyze the causes of the abnormalities, factor analysis was performed on Samples No. 1 and No. 2 and Samples No. 45 and No. 46. According to the scores of special factors, the process parameters are responsible for the inhomogenous microstructure of the four samples. The special factor score $\varepsilon=(\varepsilon_1, \varepsilon_2, \cdots, \varepsilon_{10})$ could be obtained from Eq. (1), i.e., $\varepsilon=X-\mu-AF$. The special factor score is the contribution of the ten process parameters to the final model. The factor score histogram is shown in Fig. 5. In the histogram of the special factor score, the higher bar stands for the process parameters providing greater impact on the sample no matter whether the score value is positive or negative.

As shown in Figs. 5(a) and (c), the main process variables affecting the microstructure of Sample No. 1 and Sample No. 45 are parameter numbers 3 (primary inlet water pressure), 5 (primary outlet water temperature 1) and 6 (primary outlet water temperature 2), which shows that the outlet water temperature has a significant effect on the abnormal microstructure of the cast billet. From Figs. 5(b) and (d), it can be seen that the main process variables affecting the microstructure of Sample No. 2 and Sample No. 46 are numbers 2 (temperature of liquid copper), 3 (primary inlet water pressure) and 5 (primary outlet water temperature 1). According to the above analysis, the unreasonable process parameters including the primary inlet water pressure and the primary outlet water temperature are the main reason for the abnormal microstructure.

4.5 Analysis of the causes of microstructure inhomogeneity

The measured data of the process parameters corresponding to the horizontal continuous casting copper tubular billets were further retrieved and analyzed. The curves in Figs. 6(a) and (b) are the data of primary inlet water pressure and primary outlet water temperature. The curves can be described as follows for the primary inlet water pressure and outlet water temperature.

The samples numbered in the front (1–3) and the samples numbered in the middle (44–46) fluctuate significantly from the aspects of the inlet pressure and primary outlet water temperature which are higher than the normal values compared to the other sample. From Fig. 6(a), it is obvious that the water inlet pressure of most samples is about 0.640 MPa, while the values of the samples with the front and middle numbers are higher than the normal value by about 0.027 MPa. From the above experimental results, it can also be found that a small change in the water inlet pressure can have a significant effect

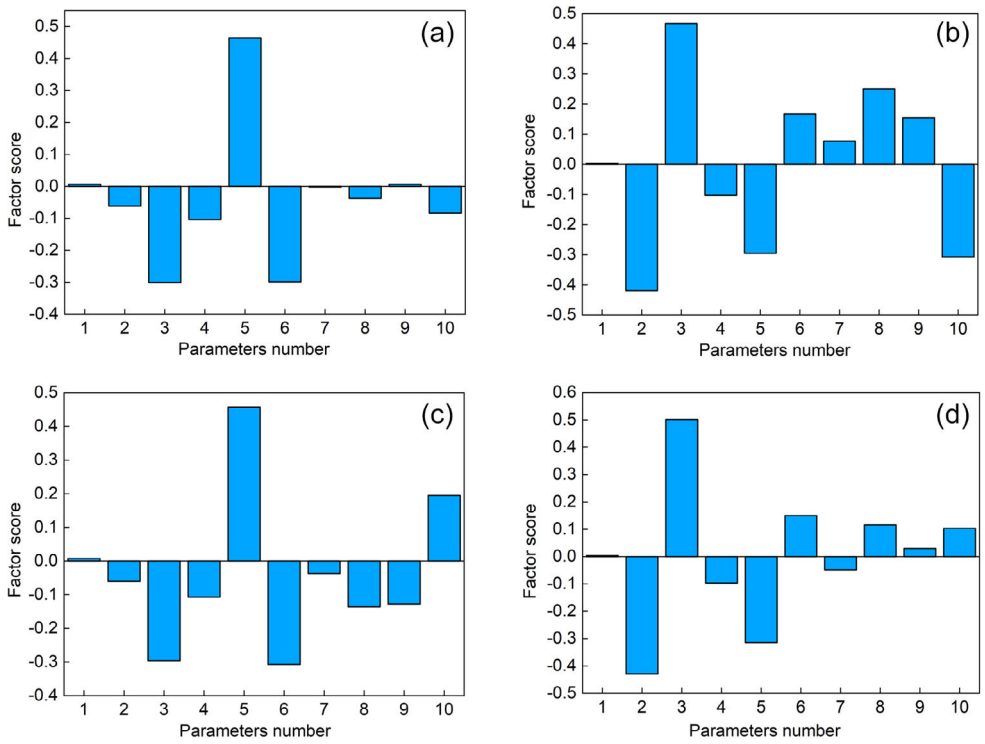

Fig. 5: Factor score histograms: (a) Sample 1; (b) Sample 2; (c) Sample 45; (d) Sample 46

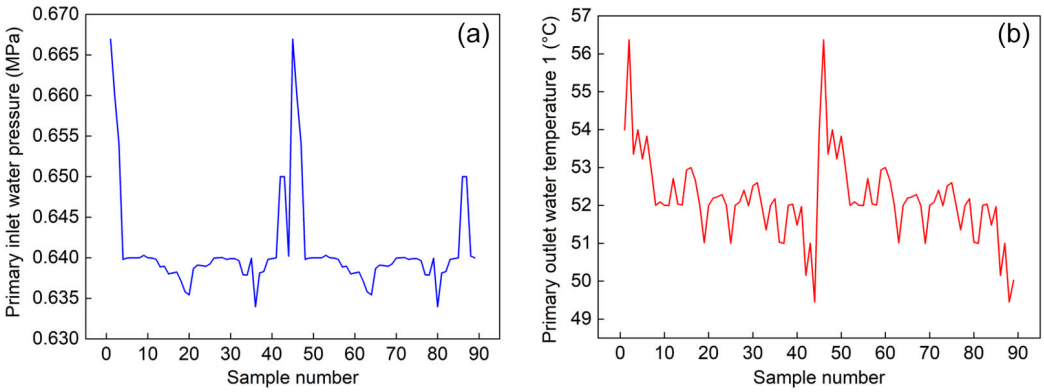

Fig. 6: Actual data curve of horizontal continuous casting process: (a) primary inlet water pressure; (b) primary outlet water temperature 1

on the billet microstructure. Therefore, special attention should be paid to control and adjust the pressure of the inlet water in the actual process. As illustrated in Fig. 6(b), it is obvious that the outlet water temperature is in the range of 51–53 °C for most of the samples, while it is in the range of 55–57 °C for the samples with the front and middle numbers.

The following analysis is conducted to reveal the relationship between the inhomogeneous cooling and the fluctuated inlet pressure of the primary pressure. As is illustrated in Fig. 7, the water flows into the main pipeline from the right side after passing the pressure sensors and the temperature sensors. During the transportation of water in the main pipeline, the layer of water close to the pipe wall will always adhere to the pipe wall, and the flow velocity distribution in the normal direction of the pipe wall shows a gradually increasing trend according to "the Law of Newton Inner Friction" [25]. Therefore, there is a velocity difference between the flow layers, which generates internal friction force under the effect of velocity gradient, causing loss along the pipeline. The loss along the pipeline increases with the distance along the pipeline according to the theory of "Energy Loss along the Route". From another aspect, vortices will generate at the point of right-angle turning when the water flows from the main pipe into the sub-pipe. Furthermore, the flow separation and the local loss will be caused due to the unexpected change of the size and direction from the main pipe to branch pipe. The further the distance from the inlet of the main pipeline, the greater the energy loss along the route. By the same token, the local loss will be greater if more right-angle turns are experienced. Therefore, the farthest branch pipe will be most affected by the fluctuation of the main pipeline, such as the "Position A" as illustrated in Fig. 7. The inlet water pressure required in continuous casting process is not stable, which affects the precision of model setting in continuous casting process resulting in the occurrence of abnormal solidification microstructures, as shown in Fig. 4.

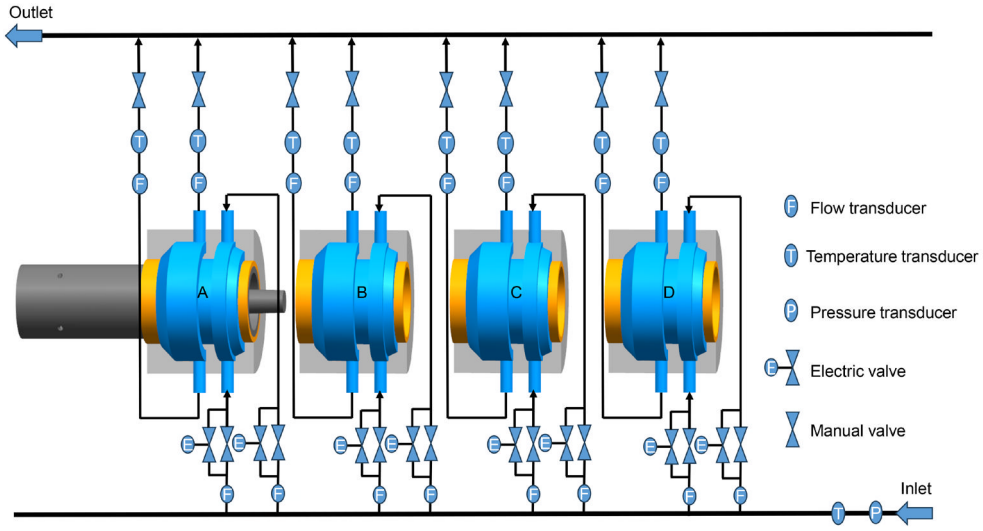

Fig. 7: Primary inlet water circuit diagram

The outlet water temperature will be unsuitable and difficult to be controlled based on the original system, namely the outlet water flow rate 1 and the outlet water flow rate 2 are both free. It means that the heat taken from upper side will possibly discord with the lower side. The heat taken away by the primary inlet water 1 in a unit time is calculated according to the heat calculation equation $Q=c\times m\times\Delta T$, which is as illustrated in Fig. 8. The sample with high outlet water temperature 1 in Fig. 6 corresponds to the sample with low heat carried according to the primary inlet water 1. This means that the sample with inhomogeneous grains as illustrated in Fig. 4 coincides with the one with lower value of the heat taken by the cooling water, as shown in Fig. 8. As it is known, the cooling effect will be weak if the heat carried is less as the primary inlet water 1 enters from the upper side. In contrast, the side with a fast-cooling rate will result in a high undercooling, a small critical nucleation radius, and an increase in the number of grains that meet the nucleation size, thereby increasing the nucleation rate. In addition, the large undercooling leads to a large difference in free energy between the solid and liquid phases, which means that the nucleation driving force is large and the crystallization speed is fast [26]. Rapid cooling weakens the diffusion ability of atoms, and the nucleated grains do not fully grow, ultimately maintaining small sizes. Therefore, the microstructure will be inhomogenous in the circumferential direction because of the inhomogeneity of temperature fields.

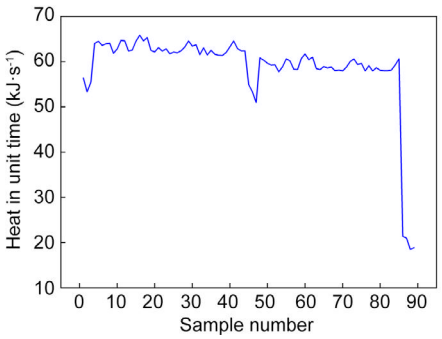

Fig. 8: Heat taken by primary inlet water 1 in unit time

Based on the above analysis, the process parameters are optimized from the following two points to prevent the generation of microstructure abnormalities:

(1) The control of the inlet water pressure: (a) A new water pump is adopted to substitute the old one to avoid the abnormal fluctuation of the inlet pressure. (b) An automatic water-cooling control system is used to control the inlet and outlet flow precisely and promptly compared with the original manual water control valve. The automatic control system of water cooling is used to precisely control the opening and closing degree of the inlet valve to guarantee the inlet water pressure to meet the requirement of the production and stable state.

(2) The control of the primary outlet water temperature: The upper and lower cooling states of the casting billet can be adjusted uniformly by changing the opening of the mechanical valve and observing the changes in the flow meter which can change the distribution ratio of primary inlet water flow rate 1 and primary inlet water flow rate 2. In this way, the temperature of primary outlet water is guaranteed to be stable and the phenomenon of inhomogeneous organization is avoided. As shown in Fig. 9, the primary inlet water flow 1 is set at about 34 $L\cdot min^{-1}$ and the primary inlet water flow 2 is about 38 $L\cdot min^{-1}$.

After optimizing and adjusting the above conditions, the data of primary inlet water pressure and primary outlet water temperature within 1 h are shown in Fig. 10. It is found that the fluctuation is significantly reduced as for the primary inlet water pressure and primary outlet water temperature 1. The primary inlet water pressure stabilizes at 0.635–0.64 MPa, and the primary outlet water temperature1 maintains at 52–53 °C.

Microstructures of the billets are homogenous and the grains are obviously refined under the optimization of the primary inlet water pressure and primary outlet water temperature 1. The equivalent width of the grains is in the range of 1–3 mm and the homogeneity of the grains is obviously enhanced, as shown in Fig. 11. The billet with qualified structure and uniform grain size can be obtained if the process parameters are suitably adjusted and kept stable based on the results of factor analysis.

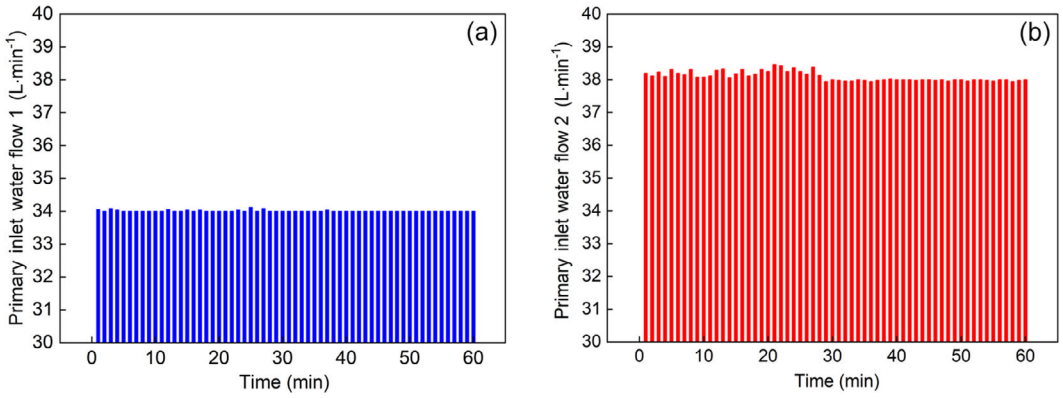

Fig. 9: Primary inlet water flow histograms: (a) primary inlet water flow 1; (b) primary inlet water flow 2

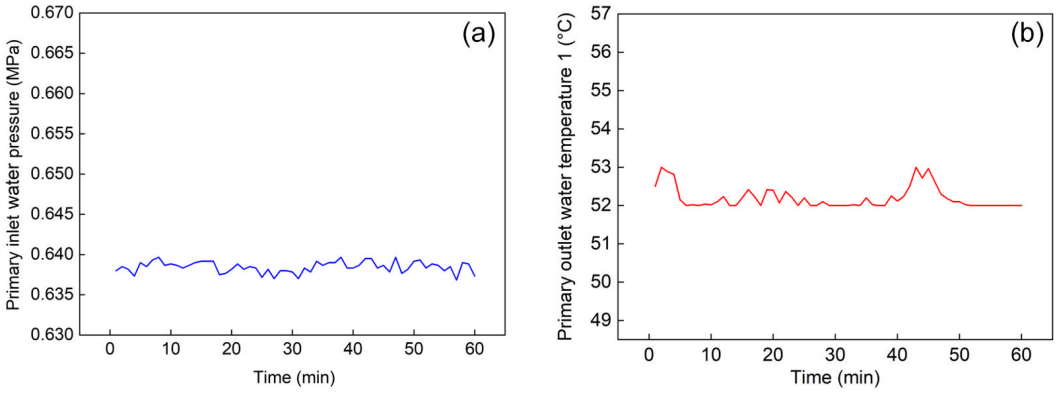

Fig. 10: Actual data curve after optimization: (a) primary inlet water pressure; (b) primary outlet water temperature 1

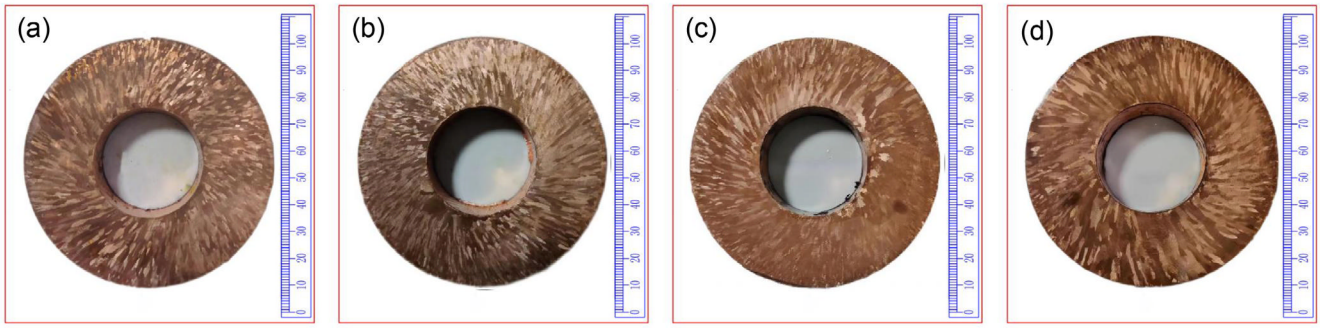

Fig. 11: Microstructure diagram after adjusting process parameters: (a) Sample 1; (b) Sample 2; (c) Sample 3; (d) Sample 4

5 Conclusions

The factor analysis method was applied to diagnose the inhomogenous microstructure of copper tubular billet by horizontal continuous casting. The process variables were classified and the microstructure abnormalities were monitored based on the factor analysis. Moreover, the causes affecting the microstructure abnormalities were analyzed and the process parameters were optimized to guarantee the production of high-quality copper billets. The following conclusions can be obtained:

(1) The 10 process parameters are represented by 3 common factors namely water flow factor, outlet factor, and control factor based on the factor rotation which can reduce the number of the variants and the complexity of the data dealing.

(2) The primary inlet water pressure and the primary outlet water temperature are the most prominent process parameters for the homogeneity of the circumferential microstructure based on the special factor analysis, namely, the inhomogenous microstructure corresponds with the unsuitable process parameters.

(3) The grain is refined and the microstructure homogeneity is obviously enhanced if the primary inlet water pressure can be controlled in the range of 0.635–0.640 MPa and the primary outlet water temperature is controlled in the range of 52–53 °C based on the investigation of the factor analysis.

Acknowledgements

This work is financially supported by Basic Scientific Project of Liaoning Provincial Department of Education (LJKMZ20220591) and Science and Technology Plan Project of Changzhou, China (CQ20220057).

Conflict of interest

The authors declare that they have no conflict of interest.

References

[1] Peltola H, Lindgren M. Failure analysis of a copper tube in a finned heat exchanger. Engineering Failure Analysis, 2015, 51: 83–97.
[2] Chandra K, Kain V, Shetty P, et al. Failure analysis of copper tube used in a refrigerating plant. Engineering Failure Analysis, 2014, 37: 1–11.
[3] Xie J X, Wang Y, Huang H Y. Extreme plastic extensibility and ductility improvement mechanisms of continuous columnar-grained copper and copper alloys. The Chinese Journal of Nonferrous Metals, 2011, 21(10): 2324–2336. (In Chinese)
[4] Edosa O O, Tekweme F K, Gupta K. Squeeze casting for metal alloys and composites: An overview of influence of process parameters on mechanical properties and microstructure. China Foundry, 2023, 20(2): 148–158.
[5] Hu X P, Zhao Y, Wang Q, et al. Effect of pouring and cooling temperatures on microstructures and mechanical properties of as-cast and T6 treated A356 alloy. China Foundry, 2019, 16(6): 380–385.
[6] Li J, Wu H T, Liu Y, et al. Solidification structure simulation and casting process optimization of GCr15 bloom alloy. China Foundry, 2022, 19(1): 63–74.
[7] Chen X Y, Fang H Z, Wang Q, et al. Microstructure and microhardness of Ti-48Al alloy prepared by rapid solidification. China Foundry, 2020, 17(6): 429–434.
[8] Zhou Z, Tan Y, Shi P. Fault detection of a sandwich system with dead-zone based on robust observer. Systems & Control Letters, 2016, 96: 132–140.
[9] Li H, Xiao D Y. Survey on data driven fault diagnosis methods. Control and Decision, 2011, 26(1): 1–9. (In Chinese)
[10] Sun F, Xu H, Zhao Y H, et al. Data-driven fault diagnosis of control valve with missing data based on modeling and deep residual shrinkage network. Journal of Zhejiang University Science A: Applied Physics & Engineering, 2022, 23(4): 303–313.
[11] Wen C L, Lv F Y, Bao Z J, et al. A review of data driven-based incipient fault diagnosis. Acta Automatica Sinica, 2016, 42(9): 1285–1299. (In Chinese)
[12] Peng L, Han G, Pagou A L, et al. Electric submersible pump broken shaft fault diagnosis based on principal component analysis. Journal of Petroleum Science and Engineering, 2020, 191: 107154.
[13] Tafarroj M M, Kalani H, Moavenian M, et al. An application of principal component analysis method in wood defects identification. Journal of the Indian Academy of Wood Science, 2014, 11: 33–38.
[14] Gu Y K, Zhou X Q, Yu D P, et al. Fault diagnosis method of rolling bearing using principal component analysis and support vector machine. Journal of Mechanical Science and Technology, 2018, 32: 5079–5088.
[15] Wang G, Liu J, Li Y, et al. Fault diagnosis of chemical processes based on partitioning PCA and variable reasoning strategy. Chinese Journal of Chemical Engineering, 2016, 24(7): 869–880.
[16] Sharifi R, Langari R. Nonlinear sensor fault diagnosis using mixture of probabilistic PCA models. Mechanical Systems and Signal Processing, 2017, 85: 638–650.
[17] Jiang Q, Yan X. Probabilistic monitoring of chemical processes using adaptively weighted factor analysis and its application. Chemical Engineering Research and Design, 2014, 92(1): 127–138.
[18] Zhao Z G, Liu F. Factor analysis and its application to process monitoring. CIESC Journal, 2007, 58(4): 970–974. (In Chinese)
[19] Liu Y Q, Li Y, Sun Z H, et al. Research on fault diagnosis of wastewater treatment process based on factor analysis. Control Engineering of China, 2015, 22(3): 447–451. (In Chinese)
[20] Ding J L, Ai H. Fault diagnosis of rotary kiln based on factorial analysis. Control and Instruments in Chemical Industry, 2019, 46(2): 115–120. (In Chinese)
[21] Peng W, Xin H S, Li X D, et al. Diagnosis of quality defects in hot strip rolled products based on factor analysis. Journal of Northeastern University (Natural Science), 2022, 43(6): 809–814. (In Chinese)
[22] He J, Ji X, Pan D. Research on economic structure of Ya'an city based on factor analysis. 2022 International Conference on Financial Market and Enterprises Management Engineering, Qingdao, 2022.
[23] Xiao Y, Han Y, Huang M, et al. Numerical calculation about influence of crystallizer structure on the stress evolution process of horizontal continuous casting of copper tubes. Journal of Pressure Vessel Technology, 2022,144(2): 021502.
[24] Han Y, Zhang X B, Yu E, et al. Numerical analysis of temperature field and structure field in horizontal continuous casting process for copper pipes. International Journal of Heat and Mass Transfer, 2017, 115: 294–306.
[25] Xiong D K. Improvement for Newton's law of viscosity and Darcy's law. Geotechnical Engineering Technique, 2004, 18(6): 275–278.
[26] Cahoon J R. On the nucleation rate for the solidification of metals. Canadian Journal of Physics, 2013, 91(2): 140–145.